Measuring minority-carrier diffusion length using a Kelvin probe force microscope

R. Shikler, N. Fried, T. Meoded, and Y. Rosenwaks
Department of Physical Electronics, Faculty of Engineering, Tel-Aviv University, Ramat-Aviv 69978, Israel
(Received 10 September 1999)

A method based on Kelvin probe force microscopy for measuring minority-carrier diffusion length in semiconductors is described. The method is based on measuring the surface photovoltage between the tip of an atomic force microscope and the surface of an illuminated semiconductor junction. The photogenerated carriers diffuse to the junction and change the contact potential difference between the tip and the sample, as a function of the distance from the junction. The diffusion length L is then obtained by fitting the measured contact potential difference using the minority-carrier continuity equation. The method was applied to measurements of electron diffusion length in GaP pn and Schottky junctions. The measured diffusion length was found to be ~ 2 μm, in good agreement with electron beam induced current measurements.

I. INTRODUCTION

Scanning probe microscopy has opened new opportunities to image semiconductor surfaces with unprecedented spatial resolution. Perhaps the most widely used scanning probe instrument is the atomic force microscope (AFM), which provides direct surface topographic images, as well as information on other tip/sample forces like friction, magnetic, and electrostatic. The Kelvin probe force microscopy (KPFM) technique has already been demonstrated as a powerful tool for measuring electrostatic forces and electric potential distribution with nanometer resolution. Due to its promise of high-spatial resolution surface potential measurements, the KPFM has found many diverse applications in recent years. The technique has been applied to materials science applications such as work-function mapping[1] and ordering in III-V compound semiconductors.[2] Kikukawa, Hosaka, and Imura have conducted surface potential measurements of silicon pn junctions,[3] and Vatel and co-workers have demonstrated potential measurements of resistors,[4] and n-i-p-i heterostructures.[5] KPFM has also proved to be effective in electrical characterization of submicron devices such as high electron mobility transistors[6] and light emitting diodes.[7] In addition, several groups have used the technique for two-dimensional surface dopant profiling,[8] and were able to distinguish relative changes in dopant concentration with lateral resolution of less than 100 nm.

The study of carrier transport and diffusion in semiconductors is a mature subject. The three most widely used methods for measuring diffusion lengths are electron-beam induced currents (EBIC),[9] surface photovoltage (SPV),[10] and photoluminescence (PL).[11] In the EBIC method a p-n junction or a Schottky barrier is viewed edge on. With the scanning electron microscope in a line scan mode, the electron beam scans the semiconductor perpendicular to the potential barrier and generates electron-hole pairs. The generated charge carriers then diffuse to the junction, where the electrons and holes are separated and a current is generated in the external circuit. This current, referred to as the EBIC current, reflects the amount of excess carriers generated. A theoretical fit to the experimentally measured current allows for the evaluation of L. The main disadvantage of the EBIC technique is that the shape of the EBIC curve depends on several additional factors apart from L, most importantly on the surface recombination velocity (SRV) of the surface on which the beam impinges. Several theoretical models have been derived to overcome this problem.[12]

In the SPV method, a super-band-gap energy monochromatic light of a wavelength λ illuminates the semiconductor. The intensity of the light I is changed in order to keep the measured photovoltage (which is proportional to the concentration of the minority carriers available by the surface) constant. Under certain assumptions[10] an I versus λ curve of the form $I=C[1/\alpha(\lambda)+L]$ (where C is a constant) is obtained. Combining the $I(\lambda)$ results with the knowledge of the $\alpha(\lambda)$ dependence enables the extraction of L. Hence, the main disadvantage of the SPV technique is that it requires an accurate knowledge of the $\alpha(\lambda)$ dependence of the measured semiconductor. The PL technique is based on measuring the minority-carrier lifetime,[13] and calculating L based on the measured mobility of the sample. Recently, near-field scanning optical microscopy has been used to measure L with high resolution.[14,15]

In this work we present a method for measuring minority-carrier diffusion length using KPFM. It is based on measuring the surface photovoltage between the tip of an atomic force microscope and the surface of an illuminated semiconductor junction. The photogenerated carriers diffuse to the junction and change the contact potential difference between the tip and the sample, as a function of the distance from the junction. The diffusion length L is then obtained by fitting the measured contact potential difference using the minority-carrier continuity equation. The method is applied to measurements of electron and hole diffusion lengths in GaP epilayers.

II. EXPERIMENT

The KPFM setup is based on a commercial AFM (Autoprobe CP, Park Scientific Instruments, Inc.) operating in noncontact mode. For topographic imaging, the cantilever, heavily doped silicon with sharpened tip ($R<20$ nm), was driven by a piezoelectric bimorph at a frequency (typically

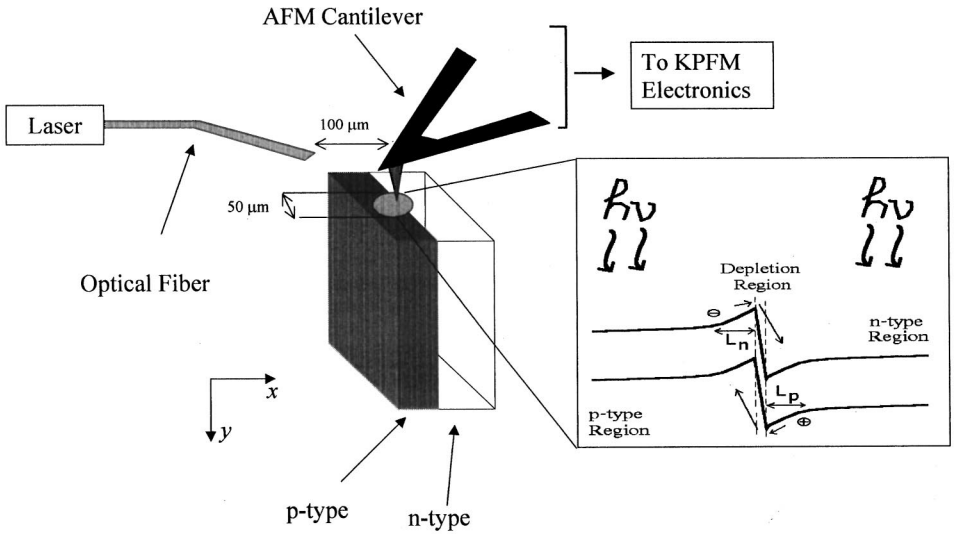

FIG. 1. Schematic diagram of the diffusion length measurement setup. The inset shows the *pn* junction band diagram under illumination, and the minority-carrier diffusion to the junction.

80–100 kHz) slightly above resonance. An alternating voltage $V_{ac}\sin(\omega t)$ at a frequency of around 20 kHz was applied to the cantilever in order to induce an electrostatic force between the tip and the sample. The contact potential difference (CPD) between the tip and the sample surface was measured in the conventional way by nullifying the output signal of a lock-in amplifier that measures the electrostatic force at the frequency ω.[1]

The GaP samples used in this study (Elma Inc.) were grown by liquid-phase epitaxy. They consisted of either $p/n^+/n$ or $n/p^+/p$ structures of a 10–13 μm-thick Zn-doped GaP ($p \simeq 5\times10^{17}$ cm^{-3}) layer on top of a 40-μm-thick *n*-type layer grown on a GaP *n*-type substrate. Ohmic contacts were formed using evaporation of Ni/Ga/Au/Ni/Au for the *n*-type layers, and Pd/Zn/Pd for the *p*-type layers.

The method for measuring *L* is schematically described in Fig. 1. The GaP samples were cleaved in air and then placed in a specially designed holder for the diffusion length measurements. The cleaved or cross-sectioned semiconductor junction is uniformly illuminated from the top using a laser beam ($\lambda = 488$ nm) passing through an optical fiber brought to a distance of about 100 μm from the AFM tip. The distance between the fiber and the sample surface (which is a few nanometers underneath the tip in the noncontact operation mode) is adjusted in order to create a laser spot size much larger than the measured carrier diffusion length. In the measurements reported here a spot size of about 50 μm in diameter was used.

Figure 2 shows two CPD images (5×5 μm) of a *pn* junction measured in the dark [Fig. 2(a)], and under super-band-gap illumination [Fig. 2(b)]. It is observed that the junction built-in voltage in Fig. 2(b) is greatly reduced due to the photovoltaic effect. In addition there are two regions in Fig. 2(b) where the SPV changes exponentially with the distance from the junction edges; this is due to minority-carrier

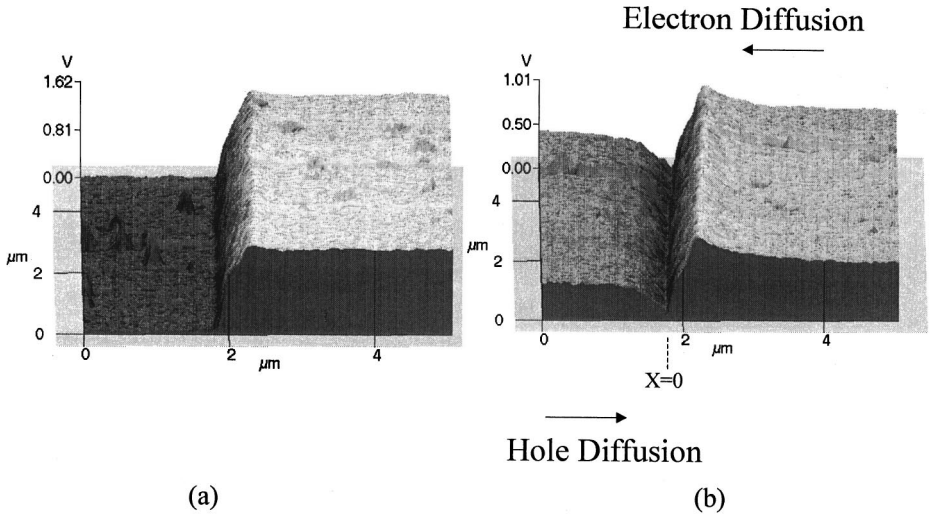

FIG. 2. Two-dimensional CPD images of the cleaved GaP *p-n* junction in the dark (a), and under super-band-gap ($\lambda = 488$ nm) illumination (b). The minority-carrier diffusion on both sides of the *p-n* junction can be clearly observed in (b).

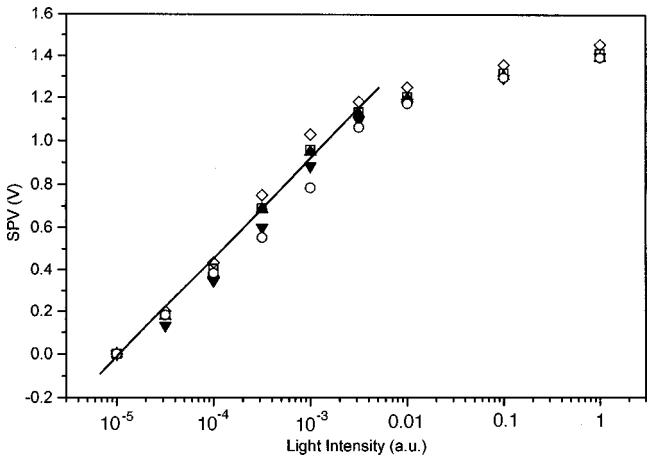

FIG. 3. Surface photovoltage measured under different light intensities; each symbol represents measurements conducted at a different position on the cleaved surface, i.e., at a different distance from the edge of the pn depletion region (in the range of 0.5–3 μm).

diffusion to the two junction edges. The bumps in the CPD image measured in the dark [Fig. 2(a)] may be due to surface states on the cleaved crystal surface.

III. ANALYSIS

The analysis of the results is based on the transport of the photogenerated minority carriers. The carriers change the CPD between the tip and sample by changing the surface band bending. The induced SPV (defined here as $|\mathrm{CPD}_{\mathrm{light}} - \mathrm{CPD}_{\mathrm{dark}}|$) is a function of the excess minority-carrier concentration. Therefore, the SPV will be the smallest at the edge of the junction (due to a depletion of the minority carriers) and will increase with the distance from the junction. The resulting SPV profile is dictated by the minority-carrier diffusion.

The calculation of the minority-carrier diffusion length from the SPV data is as follows. The dependence of SPV on Δn_{SCR} [the excess minority-carrier concentration at the edge of the cleaved surface space charge region (SCR), i.e., $\Delta n(x,y=w)$ where w is the width of the cleaved surface SCR] is obtained by measuring the SPV as a function of the exciting light intensity I. The SPV is then fitted to

$$\mathrm{SPV} = C[\ln(1 + I/I_0)]. \tag{1}$$

This equation is frequently used to relate the SPV to super-band-gap illumination intensity.[11] I_0 is an arbitrary light intensity used for normalization, and C is a constant needed for units conversion. Since Δn_{SCR} is linear with the exciting light intensity (I),[10] Eq. (1) represents the dependence of continuity equation, and substituting it in Eq. (1) above. Figure 3 shows the SPV measured under different light intensities; each symbol set represents measurements conducted at a different position on the cleaved surface, i.e., at a different distance from the edge of the pn depletion region ($x=0$ Fig. 2). The figure shows that the dependence of SPV on Δn_{SCR} does not change with the distance from the pn junction; this

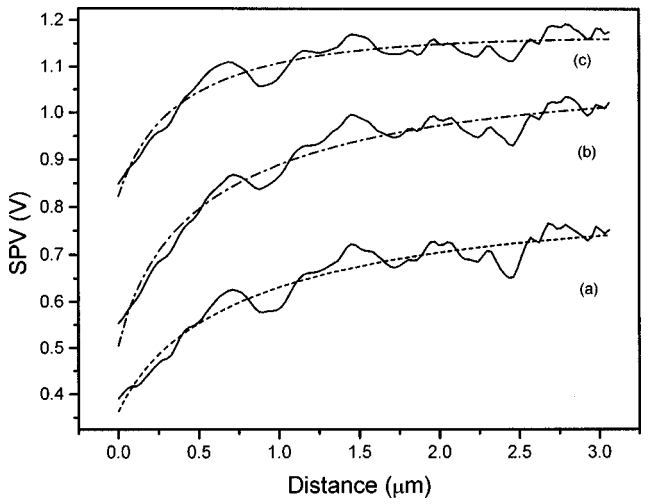

FIG. 4. Experimental (solid lines), and calculated (dashed lines) SPV profiles as a function of the distance from the edge of the pn junction ($x=0$), for three different light intensities of (a) 0.41, (b) 1.3, and (c) 4.1 μW at the output of the optical fiber. The theoretical fits based on Eq. (6) gave electron diffusion lengths of 0.85 ± 0.01, 2.1 ± 0.02, and 2 ± 0.02 μm for (a), (b), and (c), respectively.

justifies the use of Eq. (1) at all distances from the junction. A nonlinear fit to this data gives the value of the constant C in Eq. (1).

The steady-state continuity equation for electrons in one dimension (the x axis in Fig. 1), assuming uniform excitation (which is a very good assumption as long as the exciting spot size $\gg L$) can be written as

$$\frac{d^2 \Delta n_{\mathrm{SCR}}(x)}{dx^2} - \frac{\Delta n_{\mathrm{SCR}}(x)}{L_n^2} = -\frac{g}{D_n}, \tag{2}$$

where D_n is the electron diffusion constant and g is the generation function. The electric field is neglected in Eq. (2) because Δn_{SCR} is calculated only outside the junction depletion regions. This also holds for the y direction (perpendicular to the cleaved surface, see Fig. 1), which means that our calculation is valid only outside the SCR, i.e., at a distance of about 50 nm below the cleaved surface. Diffusion in the y direction is neglected because the GaP absorption depth is $(\sim 20\ \mu\mathrm{m}) \gg L_n$ for the laser wavelength used in our measurements. The solution to Eq. (2) subjected to the boundary conditions

$$\left.\frac{d\Delta n_{\mathrm{SCR}}}{dx}\right|_{x=0} = \frac{S}{D}\Delta n_{\mathrm{SCR}}(x=0), \quad \left.\frac{d\Delta n_{\mathrm{SCR}}}{dx}\right|_{x\to\infty} = 0 \tag{3}$$

is

$$\Delta n_{\mathrm{SCR}}(x) = A \exp(-x/L) + g\tau, \tag{4}$$

where τ is the effective electron bulk recombination lifetime, and A is a function of the electron velocity at the edge of the pn junction S given by

$$A = \frac{-S}{S + D/L} g\tau. \tag{5}$$

By substituting Eqs. (4) and (5) in Eq. (1), we obtain

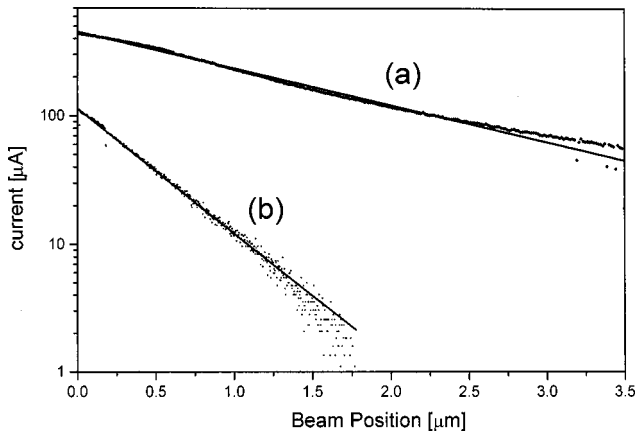

FIG. 5. EBIC profiles measured on the p side of the junction at two electron beam energies of (a) 30 and (b) 10 keV, respectively. The solid lines are qualitative fits based on an exponential decay of the EBIC profiles. They resulted in diffusion lengths of 1.5 and 0.44 μm for (a) and (b), respectively.

$$\mathrm{SPV}(x) = C \ln\{1 + [A \exp(-x/L) + g\tau]/\Delta n_0\}, \qquad (6)$$

where Δn_0 is a normalization factor.

A. Measurements on GaP *pn* junctions

Figure 4 shows experimental (solid lines) and calculated (dashed lines) SPV line scans measured under three different light intensities of (a) 0.41, (b) 1.3, and (c) 4.1 μW at the output of the optical fiber. The coordinate $x=0$ corresponds to the edge of the depletion region, see Fig. 2(b). The highest light intensity is estimated to be not more than a few μW/cm^2 exciting the sample surface under the tip. This corresponds to $\Delta n < 1\times10^{12}$ cm^{-3}, which means that all our measurements are conducted under very low injection levels. A nonlinear fit of the data to Eq. (6) with $D=3$ cm^2/s, gives an L of 0.85 ± 0.01, 2.1 ± 0.02, and 2 ± 0.02 μm, and an S of 1.7×10^5, 2.5×10^5, and 1.3×10^5 cm/s for (a), (b), and (c), respectively.

Two advantages of this method are that the measured diffusion lengths are independent of the surface recombination velocity on the cleaved surface, and of the minority carrier velocity, at the junction edges S. The surface recombination of the cleaved surface will affect the value of $\Delta n_{\mathrm{SCR}}(x)$; the larger the surface recombination, the smaller is the SPV. S will change the value of the constant A in Eq. (5), but not the decay profile of $S(x)$, which is governed by L. In addition, the fits in Fig. 4 show that (a) the values of L are not very sensitive to the carrier injection levels, (2) the value of S can be obtained from the measurements, and (3) the diffusion lengths are in excellent agreement with literature reported values for GaP; these vary between 0.5–5 μm depending upon doping and growth methods.[16]

Figure 5 shows the results of EBIC measurements conducted on the same sample for electron beam energies of 30 (a), and 10 keV (b), respectively. The solid liens are quantitative fits based on an exponential decay of the EBIC profiles, which resulted in diffusion lengths of 1.5 and 0.44 μm for (a) and (b), respectively. In general, the shapes of the EBIC curves depend on many factors.[9] Most importantly they are greatly influenced by the volume in which the excess carriers are generated (a volume of radius R) and the recombination velocity of the surface on which the beam impinges (SRV). If it assumed that the electric field outside the SCR is negligible, the transport of the generated minority carriers is purely diffusive. Under this condition, and if $S=0$, the EBIC will decrease exponentially with increasing distance x from the junction as $I(x,y)=I(0)\exp(-x/L)|_{y=\mathrm{const}}$ where y is the axis perpendicular to the surface as in Fig. 1. The effect of R is significant when its value becomes comparable to the value of L. This is the case in our measurements where R is calculated to be 6.6 and 1.05 μm for the beam energies of 30 and 10 keV, respectively. For electron beam energies of less than 10 keV, the EBIC was too small to obtain a reasonable signal-to-noise ratio. In summary, it is demonstrated that for diffusion lengths in the range of $\leqslant 2$ μm the proposed KPFM method is advantageous relative to EBIC.

B. Measurements at GaP/metal junctions

Figure 6 shows two CPD images (12×12 μm) of a metal/p-type GaP junction measured in the dark [Fig. 6(a)], and under super-band-gap illumination [Fig. 6(b)]. It is ob-

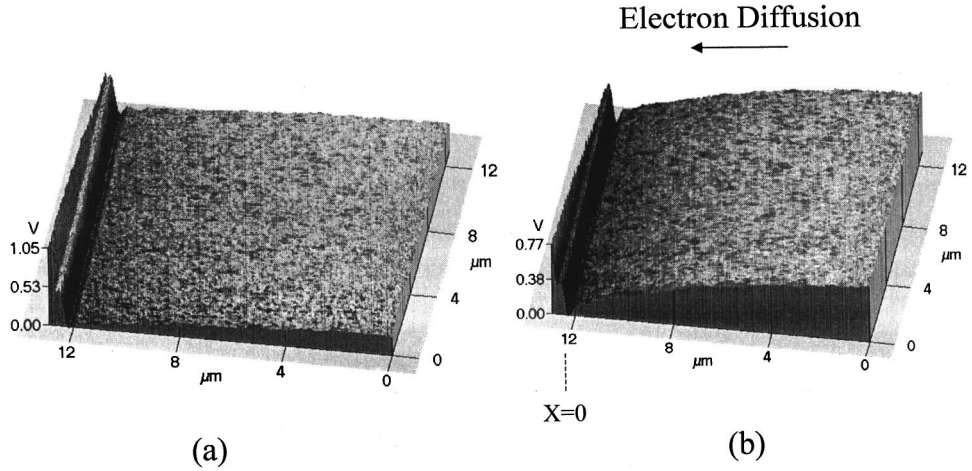

FIG. 6. Two-dimensional CPD of the cleaved GaP/metal junction in the dark (a), and under super-band-gap ($\lambda=488$ nm) illumination (b). The minority-carrier diffusion can be clearly observed in (b).

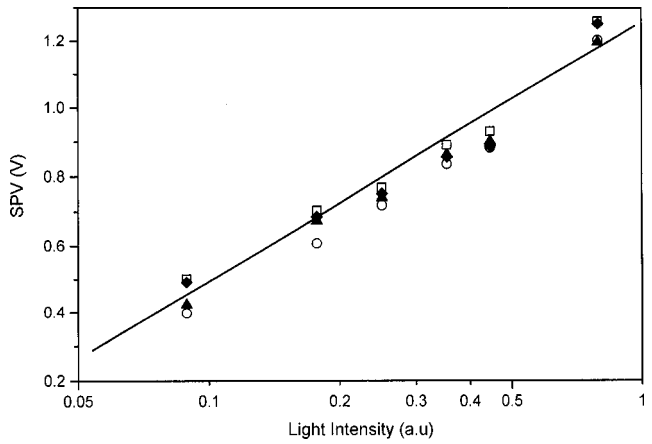

FIG. 7. Surface photovoltage measured under different light intensities; each line represents measurements conducted at a different position on the cleaved surface, i.e., at a different distance from the edge of the *p*-type GaP/metal junction (in the range of 3–10 μm).

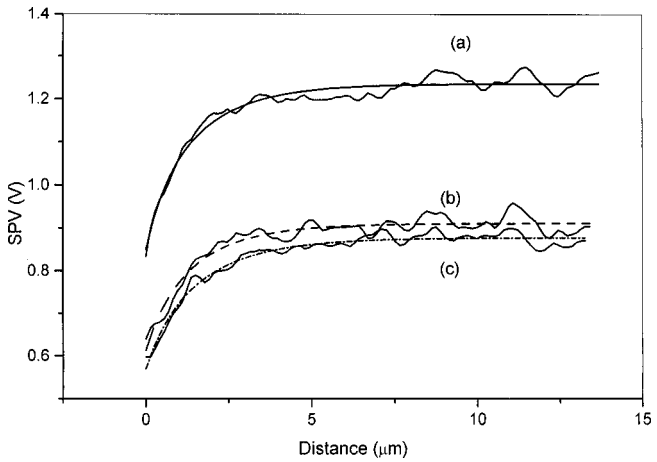

FIG. 8. Experimental (solid lines), and calculated (dashed lines) SPV profiles as a function of the distance from the edge of the junction ($x=0$), for three different light intensities of (a) 1.6, (b) 0.9, and (c) 0.71 μW at the output of the optical fiber. The theoretical fits based on Eq. (6) gave electron diffusion lengths of 1.77 ± 0.02, 1.66 ± 0.02, and 1.87 ± 0.02 μm for (a), (b), and (c), respectively.

served that the junction built-in voltage is greatly reduced due to the photovoltaic effect, but in addition there is an exponential region in the SPV image on the semiconductor side of the junction due to the carrier diffusion as in the *p-n* junction. The sharp and big potential increase observed at the position $x>12$ μm is due to the metal barrier. Figure 7 shows the SPV measured under different light intensities; each symbol set represents measurements conducted at a different position on the cleaved surface, i.e., at a different distance from the edge of the metal/*p*-type GaP junction [$x=0$ in Fig. 6(b)]. Again it is observed that the dependence of SPV on the excess carrier concentration is independent of the distance x from the edge of the *p*-type GaP/metal junction; this justifies the use of Eq. (1) for the SPV fitting at all distances from the junction.

Figure 8 shows experimental (solid lines) and calculated (dashed lines) SPV line scans measured under three different light intensities of (a) 1.6, (b) 0.9, and (c) 0.71 μW at the output of the optical fiber. The coordinate $x=0$ corresponds to the edge of the *p*-type semiconductor depletion region, see Fig. 6(b). The largest light intensity is estimated to be not more than a few μW /cm^2 exciting the sample surface under the tip. This corresponds to $\Delta n<1\times10^{12}$ cm^{-3}, which means that all our measurements are conducted under very low injection levels. A nonlinear fit of the data to Eq. (6) with $D=3$ cm^2/s, gives an L of 1.77 ± 0.02, 1.66 ± 0.02, and 1.87 ± 0.02 μm, and an S of 4.5×10^4, 4.2×10^4, and 3.9×10^4 cm/s for (a), (b), and (c), respectively. These results are in excellent agreement with the results obtained for the *pn* junctions (Fig. 4).

IV. SUMMARY AND CONCLUSIONS

We have presented a method based on Kelvin probe force microscopy for measuring minority-carrier diffusion length in semiconductors. The method is based on measuring the surface photovoltage between the tip of an atomic force microscope and the surface of an illuminated semiconductor junction. It was shown that the KPFM proposed method could be very useful in measuring very short diffusion lengths ($\leqslant2$ μm). The EBIC method is impractical for such cases, because of the volume in which the excess carriers are generated. The resolution of the KPFM technique can be below 50 nm, depending mainly on the shape of the AFM tip used in the measurements. This sets the lowest limit for diffusion length measurements using this method. In practice, this lower limit may be much larger (by a factor of 3 or more) depending on the photovoltage response of the measured sample.

The main disadvantage of the KPFM method is the lower sensitivity for narrow or medium band-gap semiconductors ($\leqslant1$ eV). This is because the SPV of a semiconductor is exponential with the band-gap energy.[17] However, since the technological importance of wide band-gap semiconductors has increased in recent years (and in most cases their diffusion lengths are very short) we believe that the KPFM method proposed here might prove to be very important.

ACKNOWLEDGMENTS

This research was supported by the Israel Science Foundation administered by the Israel Academy of Sciences and Humanities-Recanati and IDB Group foundation, and by Grant No. 9701 of the Israel Ministry of Sciences. R.S. would like to thank the Israel Ministry of Sciences for financial support.

[1] M. Nonenmacher, M. P. O'Boyle, and H. K. Wickramasing, Appl. Phys. Lett. **58**, 2091 (1991).
[2] Y. Leng, C. C. Williams, L. C. Su, and G. B. Stringfellow, Appl. Phys. Lett. **66**, 1264 (1995).
[3] A. Kikukawa, S. Hosaka, and R. Imura, Appl. Phys. Lett. **66**, 3510 (1995).
[4] O. Vatel and M. Tanimoto, Appl. Phys. Lett. **77**, 2358 (1995).
[5] A. Chavez-Pirson, O. Vatel, M. Tanimoto, H. Ando, H. Iwamura, and H. Kanbe, Appl. Phys. Lett. **67**, 3069 (1995).
[6] T. Mizutani, M. Arakawa, and S. Kishimoto, IEEE Electron Device Lett. **18**, 423 (1997); M. Arakawa, S. Kishimoto, and T. Mizutani, Jpn. J. Appl. Phys., Part 1 **36**, 1826 (1997).
[7] R. Shikler, N. Fried, T. Meoded, and Y. Rosenwaks, Appl. Phys. Lett. **74**, 2972 (1999); R. Shikler, T Meoded, N. Fried, B. Mishori, and Y. Rosenwaks, J. Appl. Phys. **86**, 107 (1999).
[8] A. K. Henning, T. Hochwitz, J. Slinkman, J. Never, S. Hoffman, P. Kaszuba, and C. Daghlian, J. Appl. Phys. **77**, 1888 (1995).
[9] R. Hakimzadeh and S. G. Bailey, J. Appl. Phys. **74**, 1118 (1993).
[10] M. Goodman, J. Appl. Phys. **32**, 2550 (1961).
[11] C. H. Wang, IEEE Trans. Electron Devices **38**, 2619 (1991).
[12] C. Donolato, Solid-State Electron. **25**, 1077 (1982).
[13] Y. Rosenwaks, Y. Shapira, and D. Huppert, Appl. Phys. Lett. **57**, 2552 (1990).
[14] A. Gustafsson, M. E. Pistol, L. Montelius,and L. Samuelson, J. Appl. Phys. **84**, 1715 (1998).
[15] A. Vertikov, I. Ozden, and A. V. Nurmiko, Appl. Phys. Lett. **74**, 850 (1999).
[16] Z. Yuanxi in *Semiconductors and Semimetals* (Academic, New York, 1988), Vol. 26, p. 44.
[17] H. G. Gatos and J. Lagowski, J. Vac. Sci. Technol. **10**, 130 (1973).